scientific reports

OPEN

Proposal for a destructive controlled phase gate using linear optics

S. U. Shringarpure✉ & J. D. Franson

Knill, Laflamme, and Milburn showed that linear optics techniques could be used to implement a nonlinear sign gate. They also showed that two of their nonlinear sign gates could be combined to implement a controlled-phase gate, which has a number of practical applications. Here we describe an alternative implementation of a controlled-phase gate for a single-rail target qubit that only requires the use of a single nonlinear sign gate. This gives a much higher average probability of success when the required ancilla photons are generated using heralding techniques. This implementation of a controlled-phase gate destroys the control qubit, which is acceptable in a number of applications where the control qubit would have been destroyed in any event, such as in a postselection process.

A controlled-phase gate produces a phase shift ϕ when the control and target qubits both have a logical value of 1. This is a very useful operation since it is a universal gate for quantum computation when combined with single-qubit operations[1]. It can also be used to create Schrodinger cat states[2], to perform nonlocal quantum interferometry with violations of Bell's inequality[3,4], and to implement complete Bell state measurements in quantum teleportation[5,6], for example.

Knill, Laflamme, and Milburn (KLM)[7] showed that linear optics techniques could be used to implement a nonlinear sign gate. They also showed that two of their nonlinear sign gates could be combined to implement a controlled-phase gate. In this paper, we propose an alternative implementation of a controlled-phase gate for a single-rail target qubit that only requires a single nonlinear sign gate. Since each operation of a nonlinear sign gate requires an ancilla photon, our approach requires one less ancilla photon than earlier approaches[7,8]. This gives a higher average probability of success when the required ancilla photons are generated using down-conversion and heralding techniques. The increased probability of success comes at the expense of destroying (erasing) the control qubit.

Logic gates in which the control qubit is destroyed have been used in a number of previous applications. For example, a destructive Controlled-NOT (CNOT) gate can be combined with a quantum encoder to implement a non-destructive CNOT gate[9–11]. The same devices can be used to implement fusion gates that allow the construction of a cluster state[12]. As another example, Bell's inequality can be violated in nonlocal interferometer experiments in which a controlled-phase shift is combined with homodyne measurements[4]. The control qubit is destroyed in a postselection process in experiments of that kind, which allows the use of the controlled-phase gate described here.

There have been several demonstrations of controlled logic operations in the coincidence basis using dual-rail qubits or polarization encoding, including controlled-phase gates[10,13,14]. However, the coincidence basis cannot be used for the single-rail target qubits of interest in this paper due to the superposition of the $|0\rangle$ and $|1\rangle$ Fock states in the input, which causes the total number of photons to be uncertain. The use of a single-rail target qubit is required for certain applications, such as in the interferometer of Ref.[3]. In addition, postselection in the coincidence basis often destroys both the control and target qubits, whereas the event-ready approach described here only destroys the control qubit. Controlled phase gates for quantum computation applications have also been achieved using nonlinear interactions with trapped atoms[15–18], for example. In contrast, the controlled phase gate described here uses only linear optical elements.

Nonlinear sign gate

The nonlinear sign gate shown in Fig. 1 is the basic building block of the KLM approach to linear optics quantum computing[1]. The input state $|\psi_{in}\rangle$ is limited to at most two photons. The operation of the nonlinear sign gate is then defined by

Physics Department, University of Maryland Baltimore County, Baltimore, MD 21250, USA. ✉email: saurabh.s@umbc.edu
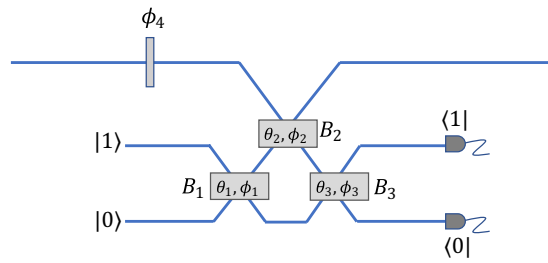
Figure 1. KLM nonlinear sign gate[7]. An input state of the form $|\psi\rangle = \alpha|0\rangle + \beta|1\rangle + \gamma|2\rangle$ gives an output state $\alpha|0\rangle + \beta|1\rangle - \gamma|2\rangle$ for an appropriate choice of the transmission coefficients of the three beam splitters $B_1, B_2,$ and B_3, along with a fixed phase shift ϕ_4. The results are heralded on the presence of a single photon in one of the two single-photon detectors.
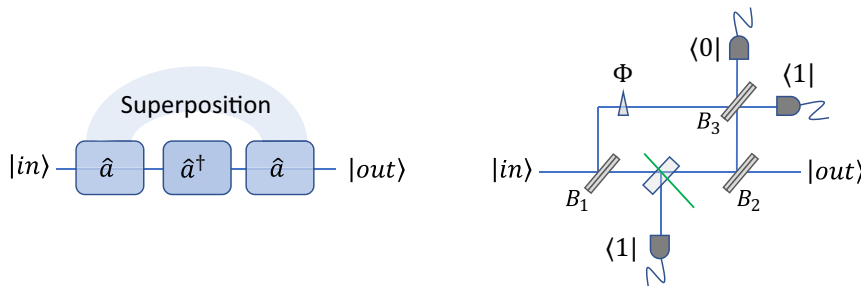

Figure 2. Alternative nonlinear sign gate suggested by Costanzo et al[19]. A superposition of $\hat{a}\hat{a}^\dagger$ and $\hat{a}^\dagger\hat{a}$ operations is implemented using photon subtraction that occurs either at the first beam splitter B_1 or at the second beam splitter B_2. These operations cannot be distinguished when a single photon is detected in one of the outputs of the third beam splitter B_3. Photon addition is implemented in between B_1 and B_2 with the aid of a heralding signal from a down conversion process. A variety of nonlinear phase shifts can be achieved by adjusting the reflectivities of the three beam splitters along with an additional phase shift Φ.

$$|\psi_{in}\rangle = \alpha|0\rangle + \beta|1\rangle + \gamma|2\rangle \rightarrow \alpha|0\rangle + \beta|1\rangle - \gamma|2\rangle, \tag{1}$$

where $\alpha, \beta,$ and γ are complex constants. The only effect of the nonlinear sign gate is to reverse the sign of the two-photon amplitude, which is similar to the effects of a nonlinear Kerr medium[19].

The KLM nonlinear sign gate utilizes three beam splitters, one ancilla photon, and postselection based on the output of two single-photon detectors, as shown in Fig. 1. The gate applies a nonlinear phase shift of π as in Eq. (1) for an appropriate choice of beam splitters and linear phase shifters as shown in Fig. 1. Other choices of the parameters can also be used to implement a nonlinear phase shift of $\pi/2$, for example[7]. There have been several proposals to enhance the success rate of this gate at the expense of adding more resources[20,21] or vice-versa[22].

Costanzo et al.[19] proposed an alternative implementation of a nonlinear sign gate that is shown in Fig. 2. As illustrated in the upper part of the figure, the device produces a coherent superposition of photon subtractions that occur either before or after a photon addition. The operation of the gate can be intuitively understood from the commutation relation $[\hat{a}, \hat{a}^\dagger] = 1$. This gate can be implemented using a down-conversion crystal with heralding to produce the photon addition, with photon subtraction occurring either at the first beam splitter B_1 or the second beam splitter B_2. Heralding on the output of beam splitter B_3 ensures that there is a fixed phase relationship between the two ways in which the photon subtraction can occur. The final state in this approach undergoes a noiseless amplification[19] in addition to the nonlinear sign shift. If necessary, this can be compensated using noiseless attenuation[23,24].

Our destructive controlled-phase gate could be implemented using either the KLM nonlinear sign gate or the alternative implementation shown in Fig. 2. Our goal is to implement a controlled phase shift using only linear optical elements, whereas the approach shown in Fig. 2 is based on the use of a nonlinear crystal. As a result, we will assume that the KLM approach is used for the nonlinear sign gate throughout the rest of this paper.
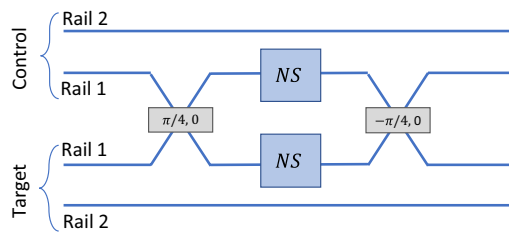
Figure 3. KLM Controlled-phase gate[7]. Dual-rail encoding is combined with Hong-Ou-Mandel interference at the first beam splitter to apply a phase shift of π if both qubits have a logical value of 1. Two nonlinear sign gates labelled NS are required.
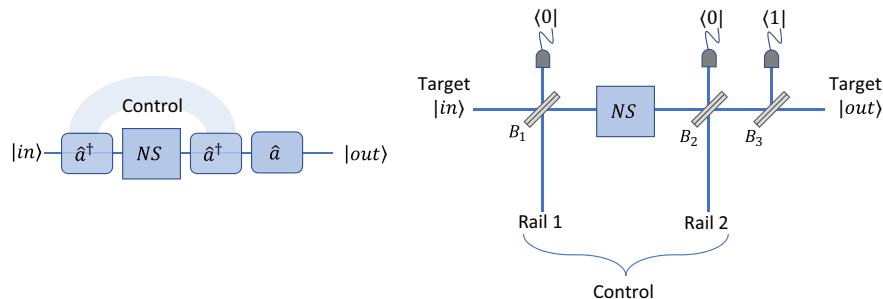

Figure 4. Destructive controlled-phase gate. Implementation of a destructive controlled-phase gate that only requires a single nonlinear sign gate labelled NS. If the control qubit has a logical value of 1, it produces a photon addition at beam splitter B_1. If the target qubit also has a logical value of 1, two photons will then pass through the nonlinear sign gate and produce a phase shift of π. In all other cases, at most a single photon passes through the nonlinear sign gate and there is no effect on the state of the system. A photon subtraction at beam splitter B_3 restores the original number of photons to the target qubit. The events are heralded on the outputs shown in three single-photon detectors. The detector in one of the output ports of beam splitter B_3 is assumed to be a photon-number resolving detector.

KLM controlled-phase gate

The controlled-phase gate suggested by KLM is shown in Fig. 3. Dual-rail encoding is used for both qubits, and the two paths corresponding to a logical value of 1 are fed into a 50/50 beam splitter. Both outputs of the first beam splitter are passed through a nonlinear sign gate, after which they are recombined on a second beam splitter to form the output of the device.

The operation of this device can be understood as being due to Hong-Ou-Mandel interference[25] at the first beam splitter. If both qubits have a logical value of 0, then no photons pass through the nonlinear sign gates and the device has no effect. If only one qubit has a logical value of 1, then a single photon passes through one of the nonlinear sign gates, which also has no effect. But if both qubits have a value of 1, then both of them will emerge in the same path after the first beam splitter as in the Hong-Ou-Mandel interferometer. In that case, one of the nonlinear sign gates will apply a phase shift of π as desired. The second beam splitter can be viewed as implementing the inverse of the Hong-Ou-Mandel interferometer with a single photon emerging in each path.

Other nonlinear phase shifts, such as $\phi = \pi/2$, can be produced by adding fixed phase shifts and varying the reflectivities of the beam splitters in the nonlinear sign gate from Fig. 1. E. Knill[8] has also described a somewhat a different implementation of a controlled-phase gate that also requires two ancilla photons as a resource.

Destructive controlled-phase gate

An alternative implementation of a controlled-phase gate that only requires a single nonlinear sign gate is shown in Fig. 4. In this case, we assume that a dual-rail encoding is used for the control qubit while a single-rail encoding is used for the target qubit. The two paths for the control qubit are incident on beam splitters B_1 and B_2, whose outputs are postselected on the absence of a photon to produce a photon addition at one of the two beam splitters. The path representing a logical value of 1 for the control qubit is assumed to be on the left-hand side of the figure, where it passes through beam splitter B_1. A nonlinear sign gate is placed between the two beam splitters, after which beam splitter B_3 is used to subtract a photon.

The initial states $|\psi_T\rangle$ and $|\psi_C\rangle$ for the target and control qubits, respectively, will be denoted by

$$|\psi_T\rangle = \alpha|0_T\rangle + \beta|1_T\rangle, |\psi_C\rangle = \gamma|0_C\rangle + \delta|1_C\rangle, \tag{2}$$

where α, β, γ, and δ are complex constants. Here $|0_T\rangle$ and $|1_T\rangle$ represent the state of the target qubit containing zero or 1 photons, while $|0_C\rangle$ and $|1_C\rangle$ correspond to the dual-rail encoded states of the control qubit.
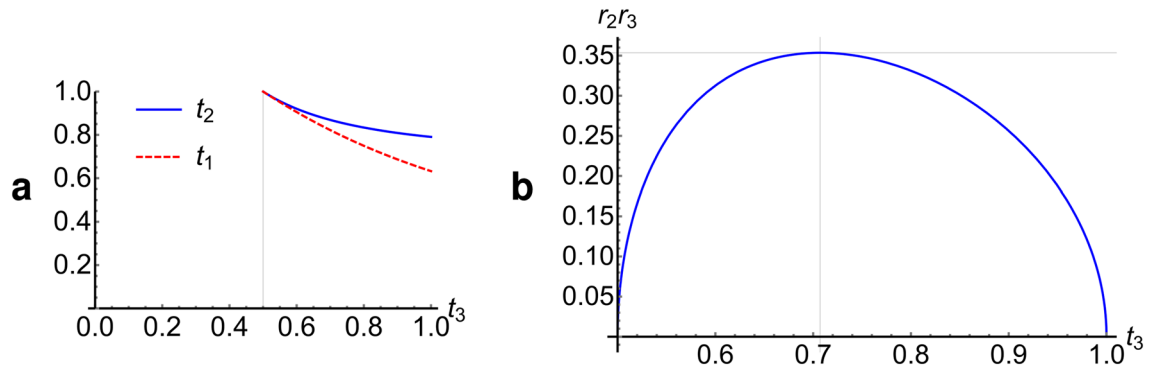
Figure 5. Parameters used in the destructive controlled-phase gate. Plots of various parameters, as a function of the transmission coefficient t_3, satisfying the conditions $2t_1t_2t_3 = 1$ and $r_2 = r_1t_2$ required for the successful operation of the destructive controlled-phase gate. (**a**) Transmission coefficient t_1 (dashed red line) and t_2 (solid blue line). The plots suggest that t_3 cannot be less than 0.5 for a solution to exist. (**b**) Product r_2r_3 that appears in Eq. (5) for the probability of success. Maxima occurs at $t_3 = 1/\sqrt{2}$, which corresponds to using a 50–50 beam splitter in the photon subtraction.

The basic idea behind the operation of the gate is illustrated in the left part of Fig. 4. If the control qubit has a logical value of 1, the photon addition occurs first and the state $|\psi'_T\rangle$ that passes through the nonlinear sign gate will contain two photons if the target qubit also has a logical value of 1. In that case, the nonlinear sign gate would produce a phase shift of π, after which the photon subtraction at beam splitter B_3 would restore the target qubit to its original number of photons. In all other cases, the state $|\psi'_T\rangle$ passing through the nonlinear sign gate would contain at most a single photon and no phase shift would be applied.

The transmission coefficients for the three beam splitters will be denoted by t_1, t_1, t_2, and t_3, while the corresponding reflection coefficients will be denoted by r_1, r_2, and r_3. If we apply the usual beam splitter transformation with a factor of i on reflection, the unnormalized state of the system at the output can be shown to be given by

$$|\psi'\rangle = (\gamma r_2 r_3[\alpha|0_T\rangle + \beta(2t_1t_2t_3)|1_T\rangle] + \delta r_1 r_3 t_2[\alpha|0_T\rangle - \beta(2t_1t_2t_3)|1_T\rangle])|0_1\rangle|0_2\rangle|1_3\rangle, \tag{3}$$

where $|0_1\rangle, |0_2\rangle$ and $|1_3\rangle$ are the states at the three detectors that herald the target output. This state does not contain the states $|0_C\rangle$ and $|1_C\rangle$ of the control qubit because it is destroyed during the heralding process.

This state can be put into the desired form by choosing the values of the transmission coefficients such that $2t_1t_2t_3 = 1$ and $r_2 = r_1t_2$. Equation (3) then reduces to

$$|\psi'\rangle = r_2 r_3[\gamma(\alpha|0_T\rangle + \beta|1_T\rangle) + \delta(\alpha|0_T\rangle - \beta|1_T\rangle)], \tag{4}$$

where we have taken the projection onto the heralded state $|0_1\rangle|0_2\rangle|1_3\rangle$. The probability of success is given by $\langle\psi'|\psi'\rangle$, which will depend on the value of the probability amplitudes in the initial state, as discussed in the next section.

Equation (3) gives a controlled phase shift of $\phi = \pi$ using the parameters described above. Other nonlinear phase shifts can be produced using different parameters in the nonlinear sign gate. It may be worth noting that the same gate can be implemented by interchanging the locations of the output target state and the third heralding detector if the transmission and reflectivity of the final beam splitter are also interchanged. The gate fidelity and the success probability will remain the same in that case because the two experimental arrangements are equivalent.

Performance comparison

The probability of success for the destructive controlled-phase gate proposed here will be compared to that of the original KLM controlled-phase gate in this section. The fidelity of both gates depends on the efficiency of the single-photon detectors used in the heralding process, and those efficiencies will also be compared.

One measure of the probability of success is to assume that the necessary ancilla photons are available with 100% probability and then calculate the intrinsic probability of success associated with the gate itself. But in many applications, the relevant probability of success would combine the intrinsic probability of success with the probability of generating the required ancilla photons using down-conversion and heralding techniques. Single photons can be generated using down-conversion with a very high fidelity, for example, which is essential in meeting the threshold for error correction.

We will first consider the probability of success for a controlled-phase gate with $\phi = \pi$. As was noted in the previous section, Eqs. (3) and (4) will give the desired result if we choose $2t_1t_2t_3 = 1$ and $r_2 = r_1t_2$, but those two equations do not completely determine the value of all three transmission coefficients. Figure 5a shows the solutions for t_1 and t_2 as a function of t_3; the solutions only exist for $t_3 > 0.5$. It can be shown that the maximum probability of success occurs for $t_1 = \sqrt{2/3}, t_2 = \sqrt{3}/2$, and $t_3 = 1/\sqrt{2}$. This gives the maximum value of the coefficient r_2r_3 that appears in Eq. (4), as can be seen in Fig. 5b.

From Eq. (4), the intrinsic probability P_D of success of the destructive controlled-phase gate is given by
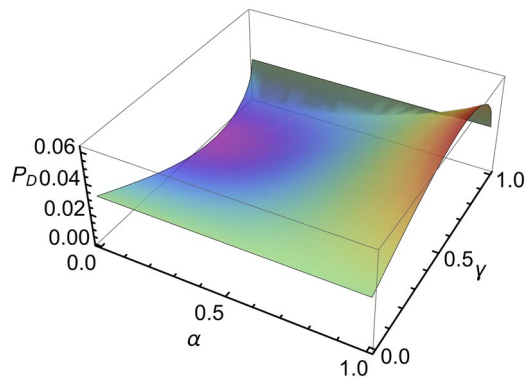
Figure 6. Intrinsic probability of success. Intrinsic probability of success P_D of the destructive controlled-phase gate as a function of the probability amplitudes α and γ in the incident control and target qubits. All four probability amplitudes in Eq. (3) were assumed to be real in this example. On the other hand, if we select β and δ to be imaginary, we get a probability independent of the real valued α and γ.

	$\phi = \pi$	$\phi = \pi/2$
P_D	0.03125	0.0226
P_{KLM}	0.0625	0.0327
P'_D	3.125×10^{-4}	2.26×10^{-4}
P'_{KLM}	6.25×10^{-6}	3.27×10^{-6}

Table 1. Comparison of the average probability of success. Here P_D and P_{KLM} are the intrinsic success probabilities of the destructive controlled-phase gate and the KLM gate respectively, while P'_D and P'_{KLM} include the probability of generating the required ancilla photons using heralded down-conversion. The nonlinear phase shift is given by ϕ.

$$P_D = P_{NSG}\langle\psi'|\psi'\rangle = P_{NSG}r_2^2 r_3^2 \left[1 + 2\left(|\alpha|^2 - |\beta|^2\right)\mathrm{Re}\left(\gamma^*\delta\right)\right]. \tag{5}$$

Here P_{NSG} is the probability of success for the nonlinear sign gate shown in Fig. 4. For the time being, we will assume that P_{NSG} is calculated based on the assumption that the ancilla photons are produced with 100% efficiency.

P_D depends on the values of the probability amplitudes α, β, γ, and δ that describe the initial control and target qubits. This is illustrated in Fig. 6, which is a plot of the intrinsic probability of success as a function of α and γ, where all of the probability amplitudes were assumed to be real with $\beta = \sqrt{1 - \alpha^2}$ and $\delta = \sqrt{1 - \gamma^2}$, for example. It can be seen that there is a significant variation in the probability of success depending on the form of the incident qubits.

If the target qubit has a logical value of 1 ($\alpha = 0$) and $\gamma = \delta$, then it can be seen from Eq. (4) that the output state will have zero amplitude and $P_D = 0$, as can be seen in Fig. 6. This is an inherent feature of a destructive controlled-phase gate where the value of the control qubit is erased. This does not occur for other values of the controlled phase shift, such as $\pi/2$, and it is not an issue in nonlocal interferometer applications, for example[3,4].

In order to simplify the comparison of the KLM controlled-phase gate and the gate proposed here, we averaged the intrinsic probability of success P_D over all possible values of the coefficients α, β, γ, and δ. This result is compared with the corresponding result P_{KLM} for the KLM controlled phase gate in Table 1. It can be seen that the intrinsic probability of success is comparable for the two gates for the case of $\phi = \pi$, which corresponds to a Controlled-Z operation.

Single photon ancilla can be generated using down-conversion and heralding on one of the pair of photons, which we will assume to succeed roughly 1% of the time[26]. Table 1 also includes the effective probabilities of success P'_D and P'_{KLM} for the two controlled phase gates if we include the probability of generating the required ancilla photons using down-conversion. It can be seen that $P'_D \gg P'_{KLM}$ since the KLM gate requires two ancilla photons while the destructive controlled-phase gate only requires a single longer ancilla photon.

As described in the previous section, a destructive controlled-phase shift of $\phi = \pi/2$ can also be produced using a different set of parameters. The KLM gate can be modified to produce a phase shift of $\phi = \pi/2$ as well[7]. The probability of success for these two gates was calculated in the same way as before and the results are also compared in Table 1. It can be seen that the destructive controlled-phase gate has a much higher average probability of success in this case as well if we include the probability of generating the required ancilla photons using down-conversion and heralding.
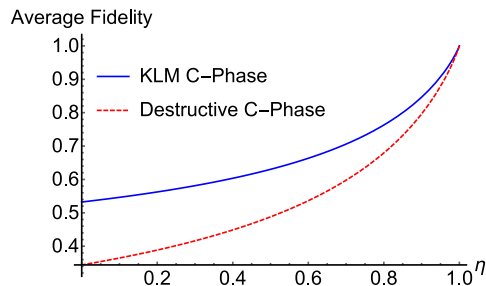
Figure 7. Comparison of the fidelities. Average fidelity F_{KLM} of the KLM controlled-phase gate (solid blue line) compared with the average fidelity F_D of a destructive controlled-phase gate (dashed red line). Both fidelities are plotted as a function of the single-photon detector efficiency η.
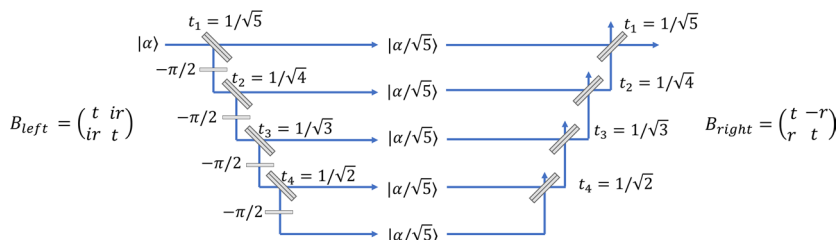

Figure 8. Controlled-phase gate for a coherent state. The incident field is divided into N separate paths, each of which contains a destructive controlled-phase gate. The case of $N = 5$ is shown here. A set of beam splitters then recombines the individual beams to form a single output state.

In principle, both types of gates can be operated with 100% fidelity if the single-photon detectors are assumed to be perfect. The dark counts in an avalanche-diode single-photon detector are typically on the order of 100 counts/second or less. With a coincidence window of 1 ns, this corresponds to an erroneous output in approximately 10^{-7} of the events, which has a negligible effect on the fidelities.

In contrast, heralding on those cases where the output of a single-photon detector indicated that no photons were present can have a significant impact on the gate fidelity if the efficiency η of the detectors is limited. Roughly speaking, this allows photons to escape unnoticed from the system, leaving an incorrect number of photons in the output state. The average fidelity F_D of the destructive controlled-phase gate of Fig. 4 and the average fidelity F_{KLM} for the KLM controlled-phase gate are plotted in Fig. 7 as a function of the detector efficiency η. Both of these results correspond to a controlled phase shift of $\phi = \pi$ and they assume that the ancilla photons have 100% fidelity.

It can be seen that the fidelity of the destructive controlled-phase gate is somewhat less than that of the KLM gate. This can be understood from the fact that the destructive controlled-phase gate of Fig. 4 relies upon 3 photon detectors indicating that no photons were detected, while the KLM gate of Fig. 3 only depends on 2 null detection events. This includes the fact that each of the nonlinear sign gates of Fig. 1 relies on a single null detection event.

The KLM gate preserves the control qubit whereas it is destroyed in the controlled-phase gate of Fig. 4. As noted previously, a destructive controlled-phase gate can be used in a number of applications, such as nonlocal quantum interference experiments, the generation of entangled Schrodinger cat states[4], and in fusion operations for generating cluster states[12]. More generally, a quantum encoder gate[9,11] could be used in combination with a destructive controlled-phase gate to preserve the value of the control qubit, but that would require an additional ancilla photon. In that case, there would no longer be any advantage in the overall probability of success as compared to using the KLM gate.

Controlled phase shift for large photon numbers

Up to now, we have assumed that the target state that is input to the controlled-phase gate of Fig. 4 contains a maximum of one photon. There are potential applications where it would be desirable to produce a controlled phase shift on a state containing a larger number of photons, such as a coherent state. This can be useful in producing Schrodinger cat states[2] or in quantum interference experiments, for example[3,4].

The controlled-phase gate can be modified as shown in Fig. 8 to allow a larger number n of photons in the input. Here a series of beam splitters is used to divide the incident field into N different paths. For $N >> n$, each of these paths will contain at most a single photon with high probability, which allows a destructive controlled-phase gate to be applied in each of the paths. The output of each of these controlled-phase gates can then be recombined using another series of beamsplitters. This approach is similar to the technique used for noiseless amplifiers when the input state has more than one photon[27].

The main limitation in this approach is that all of the controlled-phase gates have to succeed simultaneously, and the probability of that occurring decreases exponentially with the value of N. In addition, a single control qubit would need to control the phase shift in all N paths. This can be accomplished by using a series of quantum encoders[11], which would further decrease the overall success rate. Nevertheless, an approach of this kind may be feasible for relatively weak coherent states.

Summary

We have proposed a destructive controlled-phase gate that produces a phase shift of ϕ when the control and target qubits both have a logical value of 1. The most commonly used values of ϕ are π or $\pi/2$, but other phase shifts can be produced as well. The controlled-phase gate proposed here only requires a single nonlinear sign gate as a resource, whereas earlier implementations required two nonlinear sign gates[7]. As a result, the average probability of success for this controlled-sign gate is much larger than in earlier implementations if we include the need to generate ancilla photons using down-conversion and heralding. No such advantage would exist if the ancilla photons are produced on demand using quantum dots, but that typically does not give fidelities as high as can be achieved using down-conversion due to charge fluctuations[28]. Nevertheless, the use of quantum dots to produce single photons is an active area of research with continual improvements[29–31].

The basic idea behind the proposed controlled-phase gate is the use of a dual-rail control qubit to add a photon either before or after the nonlinear sign gate. If the photon is added before the nonlinear sign gate and the target qubit has a logical value of 1, then two photons will pass through the nonlinear sign gate and a phase shift of π will be produced. No such phase shift will be produced if the photon addition is done after the nonlinear sign gate. A photon subtraction is performed at the output of the gate to restore the original number of photons in the target qubit.

The increased probability of success comes at the cost of destroying the control qubit. This is acceptable in a number of applications where the control qubit would have been destroyed in any event, such as in a postselection process. Potential applications of this kind include the generation of Schrodinger cat states[2], nonlocal interference experiments that violate Bell's inequality[4], and the construction of cluster states using fusion gates[12]. The control qubit can always be preserved if necessary by using a quantum encoder circuit[11] before the controlled-phase gate, but that would require two ancilla photons and there would be no benefit as compared to the original KLM controlled-phase gate. The probability of success vanishes for certain input states for a controlled phase of π, but that is not the case for other values of the controlled phase that are required in many applications.

In summary, the controlled-phase gate described here provides an interesting example of the use of photon addition and subtraction[19], and it may be of practical use in certain applications such as the generation of Schrodinger cat states and violations of Bell's inequality.

Data availability

The Mathematica code used to generate the supporting data is available on request from the corresponding author, S.U.S.

References

1. Milburn, G. J. Quantum optical Fredkin gate. *Phys. Rev. Lett.* **62**, 2124 (1989).
2. Yurke, B. & Stoler, D. Generating quantum mechanical superpositions of macroscopically distinguishable states via amplitude dispersion. *Phys. Rev. Lett.* **57**, 13 (1986).
3. Kirby, B. T. & Franson, J. D. Nonlocal interferometry using macroscopic coherent states and weak nonlinearities. *Phys. Rev. A* **87**, 053822 (2013).
4. Shringarpure, S. U. & Franson, J. D. Generating entangled Schrödinger cat states using a number state and a beam splitter. *Phys. Rev. A* **102**, 023719 (2020).
5. Vitali, D., Fortunato, M. & Tombesi, P. Complete quantum teleportation with a Kerr nonlinearity. *Phys. Rev. Lett.* **85**, 445 (2000).
6. Paris, M. G. A., Plenio, M. B., Bose, S., Jonathan, D. & D'Ariano, G. M. Optical Bell measurement by Fock filtering. *Phys. Lett. A* **273**, 153–158 (2000).
7. Knill, E., Laflamme, R. & Milburn, G. J. A scheme for efficient quantum computation with linear optics. *Nature* **409**, 46–52 (2001).
8. Knill, E. A note on linear optics gates by post-selection. Preprint at https://arxiv.org/abs/quant-ph/0110144 (2001).
9. Franson, J. D., Donegan, M. M., Fitch, M. J., Jacobs, B. C. & Pittman, T. B. High-fidelity quantum logic operations using linear optical elements. *Phys. Rev. Lett.* **89**, 137901 (2002).
10. Pittman, T. B., Jacobs, B. C. & Franson, J. D. Demonstration of nondeterministic quantum logic operations using linear optical elements. *Phys. Rev. Lett.* **88**, 257902 (2002).
11. Pittman, T. B., Jacobs, B. C. & Franson, J. D. Probabilistic quantum encoder for single-photon qubits. *Phys. Rev. A* **69**, 042306 (2004).
12. Browne, D. E. & Rudolph, T. Resource-efficient linear optical quantum computation. *Phys. Rev. Lett.* **95**, 010501 (2005).
13. Kieling, K., O'Brien, J. L. & Eisert, J. On photonic controlled phase gates. *New J. Phys.* **12**, 013003 (2010).
14. Lemr, K. *et al.* Experimental implementation of the optimal linear-optical controlled phase gate. *Phys. Rev. Lett.* **106**, 013602 (2011).
15. Reiserer, A., Kalb, N., Rempe, G. & Ritter, S. A quantum gate between a flying optical photon and a single trapped atom. *Nature* **508**, 237–240 (2014).
16. Tiecke, T. G. *et al.* Nanophotonic quantum phase switch with a single atom. *Nature* **508**, 241 (2014).
17. Tiarks, D., Schmidt-Eberle, S., Stolz, T., Rempe, G. & Dürr, S. A photon–photon quantum gate based on Rydberg interactions. *Nat. Phys.* **15**, 124–126 (2019).
18. Liu, W.-Q., Wei, H.-R. & Kwek, L.-C. Low-cost Fredkin gate with auxiliary space. *Phys. Rev. Appl.* **14**, 054057 (2020).
19. Costanzo, L. S. *et al.* Measurement-induced strong kerr nonlinearity for weak quantum states of light. *Phys. Rev. Lett.* **119**, 013601 (2017).
20. Zou, X., Pahlke, K. & Mathis, W. Teleportation implementation of nondeterministic quantum logic operations by using linear optical elements. *Phys. Rev. A* **65**, 064305 (2002).

21. Scheel, S., Pachos, J.K., Hinds, E.A. & Knight, P.L. Quantum gates and decoherence in *Quantum Coherence*. 47–81 (Springer, Berlin, 2006).
22. Ralph, T. C., Langford, N. K., Bell, T. B. & White, A. G. Linear optical controlled-NOT gate in the coincidence basis. *Phys. Rev. A* **65**, 062324 (2002).
23. Mičuda, M. *et al.* Noiseless loss suppression in quantum optical communication. *Phys. Rev. Lett.* **109**, 180503 (2012).
24. Gagatsos, C. N., Fiurášek, J., Zavatta, A., Bellini, M. & Cerf, N. J. Heralded noiseless amplification and attenuation of non-Gaussian states of light. *Phys. Rev. A* **89**, 062311 (2014).
25. Hong, C. K., Ou, Z. Y. & Mandel, L. Measurement of subpicosecond time intervals between two photons by interference. *Phys. Rev. Lett.* **59**, 2044 (1987).
26. Meyer-Scott, E., Silberhorn, C. & Migdall, A. Single-photon sources: Approaching the ideal through multiplexing. *Rev. Sci. Instrum.* **91**, 041101 (2020).
27. Ralph, T. C. & Lund, A. P. Nondeterministic noiseless linear amplification of quantum systems. *AIP Conf. Proc.* **1110**, 155–160 (2009).
28. Kuhlmann, A. V. *et al.* Charge noise and spin noise in a semiconductor quantum device. *Nat. Phys.* **9**, 570–575 (2013).
29. Kuhlmann, A. V. *et al.* Transform-limited single photons from a single quantum dot. *Nat. Commun.* **6**, 1–6 (2015).
30. Kiršanskė, G. *et al.* Indistinguishable and efficient single photons from a quantum dot in a planar nanobeam waveguide. *Phys. Rev. B* **96**, 165306 (2017).
31. Somaschi, N. *et al.* Near-optimal single-photon sources in the solid state. *Nat. Photonics* **10**, 340–345 (2016).

Acknowledgements

Author contributions

S.U.S. and J.D.F. came up with the idea together. S.U.S. performed the calculations. Both the authors wrote and reviewed the manuscript.

Competing interests

The authors declare no competing interests.

Additional information

Correspondence and requests for materials should be addressed to S.U.S.

Reprints and permissions information is available at www.nature.com/reprints.

Publisher's note Springer Nature remains neutral with regard to jurisdictional claims in published maps and institutional affiliations.